

**Joint intensity in layered rocks:  
The unsaturated, saturated, supersaturated, and clustered classes**

Amir Sagy<sup>1</sup> and Ze'ev Reches<sup>2</sup>

Institute of Earth Sciences, Hebrew University, Jerusalem 91904, Israel

1. Current address: Department of Earth and Space Sciences, University of California, Los Angeles, CA

2. Current Address: School of Geology and Geophysics, University of Oklahoma, Norman, OK

### Abstract

We derive here a new model for joint intensity in brittle, layered rock. According to this model, joint intensity depends on the tectonic stresses, the friction between the layers, and the tensile strength of the brittle layers. For typical geologic settings of layered sedimentary rocks, the joint intensity is expected to achieve saturation when the ratio ( $D$ ) between the host layer thicknesses to the joint spacing is 1-3. On the other hand, field measurements in the western margins of the Dead Sea basin, as well as experimental observations, reveal that the ratio ( $D$ ) ranges from 0.1 to 35. Consequently, we classify the observed range of intensity into four groups: unsaturated, saturated, supersaturated, and clustered. While our model, as well as previous models, can explain the first two groups, alternative mechanisms are required to explain the second two groups. It is shown, based on our recent field and experimental analyses, that fast propagating, dynamic fractures can produce the tightly spaced patterns of the supersaturated and clustered cases.

### Introduction

The occurrence of fractures in sedimentary rocks strongly affects the mechanical and hydrological properties of the host layers. The fracture intensity ( $D$ ) in three-dimensions is the cumulative surface area of fractures within a unit volume; this value was never determined. As a two-dimensional approximation, fracture intensity can be determined by measuring the cumulative length of fractures (map view) per unit area of a map (Wu and Pollard, 1995; Reches, 1998; Sagy 1999). Many times, however, fracture intensity is estimated from one-dimensional traverse (scan-line) normal to the fractures.

Several field works (e.g Narr and Suppe, 1991; Gross, 1993; Engelder et al., 1997; Ji et al., 1998) demonstrated that mean or median joint spacing ( $s$ ) in layered rocks is often linearly related to layer thickness ( $h$ ). Furthermore, mechanical models predicted that the layer can become “saturated” with joints, and that at this stage new joints cannot form (Ji et al., 1998, Bai and Pollard, 2000). Other field works, however, display a different picture. It was shown that the intensity of joints can varies widely, from sparse occurrence to tight spacing, and in these cases there is nonlinear relations between the joint spacing and the layer thickness (Reches, 1972, 1998; Mcquillan 1973; Ladeira and Price, 1981; Sagy et al., 2001).

The present study use field observations from the western margins of the Dead Sea basin and experimental observations to explore two different mechanisms that control joint intensity in layered rocks. One mechanism, which is based on quasi-static fracturing within brittle layers, predicts linear relationship between the layer thickness, and that the saturation intensity  $D_s$  is smaller than 3;  $D_s$  is the ratio of the final fracture spacing and the thickness of the host layer. While this mechanism is in agreement with observations in many studies (e.g., Price, 1966; Hobbs, 1967; Sowers, 1973; Gross et al., 1995; Ji et al., 1998; Sagy, 1999; Bai and Pollard, 2000), it fails to explain the high joint intensity of  $D \gg 3$  found in other sites. The second mechanism is based on nonlinear processes during fast propagation of dynamic fractures (Sharon and Fineberg, 1996; Sagy et al., 2001; Sagy et al., 2004). We follow here

the common practice and use “fracture”, for tensile, mode I fractures in models and experiments, and the term “joints” for tensile fractures in the field.

## **Modeling joint intensity in layered rocks**

### **Basic concepts**

Fracturing models are usually based on a two-dimensional view of alternating brittle and ductile layers (Fig. 1). The strength of the contacts between the layers is assumed due to the bonding between elastic or viscoelastic solids (Price, 1966; Hobbs, 1967; Sowers, 1973; Gross et al, 1995; Bai and Pollard, 2000), controlled by pore fluid pressure (Ladeira and Price, 1981), or friction (Ji. et al., 1998; Sagy, 1999). These analyses assume, explicitly or implicitly, that the fractures grow by slow, quasi-static extension.

Hobbs (1967) considered fracturing within a layered sequence subjected to layer-parallel extension (Fig. 1). A fracture forms in the brittle layer when the local tensile stresses exceed the tensile strength of this layer. The formation of this fracture relaxes the tensile stresses at its proximity, thus reduces the likelihood for a new fracture to ensue and grow. Shear stresses along the layer contacts transfer extension from the ductile layers to the brittle one, and the tensile stress increases with distance from the fracture. The brittle layer fractures again wherever the tensile stress exceeds the local strength. Hobbs (1967) model and its offsprings predict that fracture intensity is proportional to the layer-parallel extension and stress intensity in the ductile (less competent) layers (Kelly and Tyson, 1965; Gross et al., 1995).

The saturation intensity can be estimated for known rock properties. Bai and Pollard (2000) used elastic stress analysis to predict saturation intensity of  $D_S \approx 0.75$ . Hobbs model predicts  $D_S \geq 2$  for unrealistic conditions in which the ductile layers are stronger by 20 times or more than the brittle one. In the next section, we present a new model for fracture intensity and fracture saturation for extensional tectonic regimes.

### **Fracture saturation in layered medium with frictional contacts**

#### Approach

The present model is based on the analysis of Kelly and Tyson (1965) for composite material built of brittle fibers embedded in a ductile matrix. According to their concept, when a composite material is subjected to extension, the matrix extends by continuous flow whereas the fiber extends elastically and by fracturing. When the composite is extended, the stress transfer from the matrix to a fiber is manifested by shear stresses along the contact between the two media. The higher tensile stresses in a fiber lead to its tensile fracturing, and the spacing between the fractures decreases until the fiber-matrix contact yields by shear. This yielding of the contact stops the fracturing of the fiber, and final fracture saturation is achieved. According to Kelly and Tyson (1965), the final fracture saturation depends on the tensile strength of the fiber and the shear strength of the contact surface.

We adopted the model of Kelly and Tyson (1965) because it fits well the fracturing processes of layered rocks, and because it requires the knowledge of only a few, well bounded mechanical parameters. The layer contacts are regarded as frictional discontinuities, and it is assumed that their friction coefficient is 0.6-0.85, according to Byerlee’s law (Byerlee, 1978; Reches et al., 1992). Thus, the shear stresses along the layer contacts can be bounded if the depth and inclination of the layers are known.

#### Model derivation

Kelly and Tyson, (1965) used force balance to show that under tension the stress,  $\sigma(x)$  at a distance  $x$  from the first fracture in the fiber depends on the shear stress along the fiber contacts,

$$1. \quad \sigma(x) = 2\tau_y \frac{x}{R}$$

where  $\tau_y$  is the shear stress along the fiber (assumed to be uniform) and  $R$  is the fiber radius. Equation (1) indicates that the tensional stress increases linearly with distance ( $x$ ), yet its magnitude must be bounded by the tensile strength of the fiber,  $T$ . A new fracture is created in the fiber at a distance ( $x$ ) in which  $\sigma(x) = T$ . Under increasing extension, this process continues to fracture the fiber with gradual decreasing spacing between the fractures (Fig. 1b). The distance between fractures reaches a critical distance,  $L_C$ , when the shear stress at the fiber contact is larger than its frictional strength of the contact,  $\tau_{yc}$ , (Fig. 1b). According to equation (1), the fiber will be disconnected from the matrix when

$$2. \quad L_C = R \frac{T}{2\tau_{yc}}$$

Equation 2 is the ‘‘Kelly Equation’’ (Roman et al., 1992), which predicts that fracture saturation intensity of the composite will occur in the range of  $L_C/2$ - $L_C$  with a mean length value of

$$3. \quad \langle L_m \rangle = \frac{3}{4} L_C$$

For the application of these concepts to the analysis of layered rock, we consider a 2D configuration with a sequence of two ductile layers with a brittle layer between them (Fig. 1a). The layers are horizontal with remote stress state of  $\sigma_v > \sigma_h$ , where the vertical stress,  $\sigma_v$ , reflects the overburden load. Both remote stresses are compressive, such as common in extensional tectonic regimes (Reches et al., 1992; Zoback, 1992). It is assumed here, similarly to the model of Kelly and Tyson, that the extension of the ductile layers is continuous and larger than the extension of the brittle layer (see also Gross et al., 1995; Reches, 1998). This larger extension of the ductile layers invokes a shear stress  $\tau_{xy}$  along the layer contacts that transfers load from the ductile layers to the brittle one.

Following our above assumption that the layer contacts behave as frictional rock interfaces, the shear stress along the contacts is

$$4. \quad \tau_{xy} \leq a\sigma_v + b$$

where  $\sigma_v$  is the normal stress component (in our configuration  $\sigma_n = \sigma_v$ ), and  $a, b$  are Byerlee’s coefficients of  $a = 0.85$  and  $b=0$  at depth of 10 km or less. Applying the force balance concept (equation 1) to the present geometry, the horizontal stress within the brittle layer at distance  $x$  from an existing fracture is,

$$5. \quad \sigma(x) = 2\tau_{xy} \frac{x}{h}$$

Near the fracture surfaces, the tensile stresses and the shear stresses between the layers are  $\sim$  zero, and they increase linearly with distance (see above). A new fracture would form when

$$6. \quad \sigma(x) = \sigma_h + T$$

where  $T$  is the tensional strength of the brittle layer. As the maximum shear stress at the layer contacts is bounded by the friction (equation 4), the critical length value (equation 2) can be determined by substituting equations 4 and 5 in equation 6 and rearranging. We find that the critical fracture spacing is,

$$7. \quad L_C = \frac{h(\sigma_h + T)}{2(a\sigma_v + b)}$$

Taking  $b=0$  in the upper 10 km of the crust (Byerlee, 1978; Reches et al., 1992), and using equation 3 for the mean spacing, we find that the saturation intensity can be written as:

$$8. \quad D_S = \frac{8}{3} \frac{a\sigma_v}{\sigma_h + T}$$

Equation 8 presents the saturation fracture intensity as function of the friction coefficient between layers (a), the tectonic stresses ( $\sigma_h$ ), and the strength of the brittle layer (T). According to our model, the rise of extension after fracture saturation would lead to shear failure and slip along the layers contacts; such slip will be similar to bedding-plane slip documented during folding (Ghosh, 1968; Reches and Johnson, 1976). It is thus expected that further extension will be accommodated by opening of existing joints, and flow or fracture of the ductile layers (Becker and Gross., 1996).

### Model application to the Dead Sea margins

We apply the above model to joint intensity measurements in dolostone layers within the western margins of the Dead Sea (Sagy et al., 2001, Sagy et al., 2003). The Dead Sea basin is bounded on its western margins by a belt of large, active faults. The belt trends N-S, it is 100 km long, 3-5 km wide and the cumulative vertical displacement along its faults exceeds 10 km. Sagy (1999) used borehole image analysis and stress inversion methods to find that the stress field in this area is extensional with  $\sigma_v > \sigma_H > \sigma_h$ . We measured fractures in stations that are located on exposures of dolostone and limestone of the Judea Group, distributed along 50 km of the belt. The present analysis is limited only to systematic joint sets in the dolostone layers (17 stations). The studied fractures were recognized as joints by their fractographic features (Bahat, 1991): concentric rib marks, and radial (plumose and hackles). Most of the measurements are based on mapping at 1:10 scale of joints exposed on top of sub-horizontal layers. In others we used scan-lines that ran 30 m to 120 m long (Sagy, 1999; Sagy et al., 2003).

Measurement in these 17 stations yielded 31 values of D, including 17 values for the dominant sets in each of the stations, and 14 values for the secondary sets. The plot of these data (Fig. 2a) reveals three distinct groups: Group A with  $D = 1.3-2.6$  for the dominant joint set in thin layers ( $h < 0.5$  m); Group B with  $D < 1$  for the secondary joint set in thin layers ( $h < 0.5$  m); and Group C with  $D > 3$ , for the layers with  $h > 0.5$  m. Note that the highest intensity in Group A is in one station with  $D = 3.5$ , located a few meters from a large normal fault.

The expected saturation intensity in this area is calculated according to the above frictional model (equation 8) and the following parameters are estimated. First, it is assumed that the pore pressure is constant in all layers, and thus the tectonic stresses are regarded as the effective stresses. Second, we assume  $\sigma_v = \rho g H$ , where  $\rho = 2,500 \text{ kg/m}^3$  is the mean rock density, and  $H = 0.3-0.7$  km is the depth range of the measured rock layers (Sagy, 1999). Third, following Byerlee's law we use  $a = 0.85$  and  $b=0$ . Fourth, we use tensile strength of  $T = 7.5 \text{ MPa}$  for dolomite rocks (Finno, 2002). Finally, we assume that the range of tectonic stress ratio,  $\sigma_h/\sigma_v$ , is from 0.3 to 0.7 as shown for example by Reches et al. (1992) and Zoback (1992).

The predicted  $D_S$  for  $\sigma_h/\sigma_v = 0.3-0.7$  (effective stresses) are plotted in Fig. 2b. The measured values of D (of groups A, B, and C) are also plotted as rectangles at the appropriate depth interval of H. This plot indicates a good agreement between measured D values and predicted  $D_S$  values: group A (the dominant joint set in each field station, Sagy 1999) fits the corresponding saturated values for the marked conditions, and group B (the less developed joint set) fits the unsaturated range of D values. However, the intensity of group C, with  $D = 8-22$ , is supersaturated and cannot be explained by the present model or by any other quasi-static models.

## Classes of joint intensity

### Observational classes

The compilation of fracture intensity observations in the field and experiments reveals that  $D$  values range from 0.1 to 35 (Fig. 3a). On this range of observed  $D$  values, we plot the band of predicted saturation intensity as  $D_S = 1.0-3.0$ , which encompasses the model predictions for a reasonable range of rock properties. This band divides the observed data into three intensity classes (Fig. 3a), which are portrayed schematically in Fig. 3b. These classes are (1) unsaturated with  $D < 1.0$ , (2) saturated with  $D = 1.0 - 3.0$ , and (3) supersaturated with  $D > 3.0$ . A fourth class, which was termed clustered (Sagy et al., 2001), or swarm (Putot et al., 2001) is displayed in Fig. 3b; this class has irregular intensity with local  $D > 3.0$  and mean  $D < 3.0$ . These four classes are characterized below by several examples.

### The saturated and unsaturated classes

Our observations of group A (Fig. 2a) join many previous field observations that demonstrated linear relationship between layer thickness and mean joint spacing, and model-predicted joint intensity. These relations are common for thin layers in many tectonic regimes and for a range of sedimentary rocks (Ladeira and Price, 1981; Ji et al., 1998). The mean  $D$  value in our results is larger than observed in other tectonic regimes (e.g. Narr, 1991; Gross, 1993). These variations can reflect the different measuring methods (Wu and Pollard, 1995), or different values of the  $\sigma_h/\sigma_v$  ratio for other tectonic regimes. Furthermore, joint interaction and rise of pore pressure, even under extensional load, could raise the local values of  $\sigma_h$  and prevent further jointing (Bai and Pollard, 2001; Germanovich and Astakhov, 2004).

The unsaturated class is represented here by secondary joint systems. In general, this class could include any joint set that is only partly developed due to low extension intensity.

### The supersaturated class, field examples

Three cases of supersaturated fracture intensity are presented below. One case is in thick layers (McQuillan 1973; Ladeira and Price, 1981), a second in thin layers (Reches, 1998), and a third of gradual systematic intensity increase within one layer in the proximity of a fault (Sagy et al., 2001).

McQuillan (1973) analyzed joint sets of Asmari Limestone in southwest Iran, an intensely folded region with Mesozoic thrust systems. He used the scan line method to measure joint intensity in hundreds of stations within a 320 km long region. McQuillan (1973) found that joint spacing is nonlinearly related to layer thickness and that the associated  $D$  values are as high as  $D \approx 11$  in 12 m thick layers. He also noted that joint intensity in the Asmari Limestone does not depend on local folding, and that very tight joints were observed in graben regions where fault-associated joints predominate. Ladeira and Price (1981) presented similar intensity relations for graywacke and sandstone layers in England and Portugal. Their results indicate  $D$  values up to 35 in layers thicker than 0.5 m.

Reches (1998) studied the joints within limestone layers of the Carmel Formation, Cedar Mountain area, central Utah (Fig. 4a). These are flat lying layers in the Colorado Plateau region, east of the San Raphael swell. The limestone layers are 0.05 to 0.75m thick and are embedded between much thicker layers of compliant siltstone, marls and shales. The limestone layers are intensely fractured by two dominant sets of sub-vertical joints; the angle between the strikes of the two sets is about  $40^\circ$ . The fracture intensity was measured in the scale-line method on horizontal or vertical surfaces, and in the cumulative-length method for maps; the calculated  $D$  values range from 3 to 34.

Sagy et al. (2001) mapped joints within a 3 m thick layer of brittle dolomite in the Ein-Gedi area, the west margins of the Dead Sea (Fig. 4b). The dolostone layer is exposed along a 120 m long sub-vertical erosional wall that was mapped at scales from 1:20 to 1:1. This exposure is bounded on the east side by a large normal fault that displaced the mapped layer by at least tens of meters. The intensity of the large joints in the exposure increases significantly toward the fault. While  $D$  is  $\approx 2.0$  at a distance of 80-100 m west of the fault, it increases to  $D \approx 22$ , at 30 m distance from the fault (Sagy et al, 2001). Detailed mapping revealed that most of the joints have a “tree-like” shape with many branches. These branches increase the surface area of a single joint by a factor of ten or more (Sagy et al., 2001). At the fault proximity, the branches of neighboring joints create a dense fracture network within a fragmented layer.

### **Supersaturated and clustered classes in laboratory experiments**

Laboratory experiments with layered composites usually yielded low values of saturation densities. Garrett and Bailey (1977) stretched a layered composite of fibers within resin and demonstrated that  $D$  increases with extension until the samples failed when  $D$  approached 1.0. Wu and Pollard (1995) bent ductile plates with thin brittle coating, and the maximum achieved intensity approached  $D = 0.15$ . In contrast to these experiments, our tests (Sagy, 1999; Sagy et al., 2001) generated high saturation densities of  $D \leq 10$ . We used layered composites made of two polycarbonate layers cemented to each other by brittle epoxy and subjected to axial extension (Fig. 5a). All four classes of fracture intensity were observed in these experiments (Sagy, 1999). We, however, present here only tests in which the epoxy behaved in a brittle mode (when the strain rates was higher than  $1 \cdot 10^{-3} \text{ sec}^{-1}$ ; Sagy et al., 2001). We describe only tests with branching fractures and tests with fracture intensity of the clustered class.

The experimental branching fractures (Fig. 5b) are composed of many short segments that split from each other with up to six forking segments at a single junction. Branches form a hierarchical structure with up to eight branching levels in the present experiments. The measured cumulative length of all observed branches in a single fracture is up to six times the length of a planar fracture across the sample.

Clustering fractures (Fig. 5c) developed under the highest strain rates of these tests, with extension rates of  $2 \cdot 10^{-3} \text{ sec}^{-1}$  to  $7 \cdot 10^{-3} \text{ sec}^{-1}$ . A clustering fracture includes several branching fractures that crosscut each other, forming a wide zone of intense fracturing. In a simple cluster each branch may be traced to its parent fracture, but complex clusters appear as integral structural units of intensely fractured zones (Fig. 5c). Further, the experiments indicate that a clustering fracture grows during a single, fast event (Sagy et al., 2001). Video records of the tests show that in a 30 mm wide sample a cluster develops in less than 0.04 sec (Reches et al., 2000). While all fractures inside one cluster develop quasi-simultaneously, whole clusters continue to fill the sample gradually as long as the axial extension increases (Reches et al., 2000). Clustering stopped due to delamination or yielding of the polycarbonate layers.

A cluster or a branching fracture includes many secondary segments with large cumulative length and enlarged surface area with respect to a planar fracture. The global fracture intensity for several clusters has two contributions: (1) the cumulative length of the fractures inside the cluster,  $L_f$ , and (2) the number of clusters,  $n$ . The fracture intensity determined in the cumulative-length method for a sample with area  $A$  is:

$$D = h (n \cdot L_f / A)$$

Our measurements inside individual clusters indicate local  $D$  values in the range of 5-13, whereas the corresponding  $D$  of the entire sample is 2.5-10. These values are about ten times higher than intensity values observed in our lower strain rate tests.

## Discussion

### Saturation of natural joints

Models of fracture intensity in layered media or composite materials suggested that the intensity should exhibit a saturation limit. First, the ductile layers can fail (Hobbs, 1967). Second, the brittle layer can be delaminated from the ductile layers, if the shear stresses along the layers contacts exceed the contact shear strength (or the ductile layers strength), (Kelly and Tyson, 1965; Garrett and Baily, 1977). Third, the existing fractures induce compressive stresses between themselves and prevent further fracturing of the brittle layer (Bai et al., 2000; Germanovich and Astakhov 2004). Based on the present compilation of field measurements (Fig. 2a, 3a) and the results of our model (Fig.2b) we suggest that saturation intensities for realistic geological cases converge to the range of  $D_S = 0.75-3.0$ . The same compilation, however, suggests that this range is relatively small with respect to the range of intensities,  $D_S = 0.1-35$ , observed in the field. We classify above the four classes of joint intensity (Figs. 2, 3): unsaturated ( $D < 1.0$ ), saturated ( $D = 1.0 - 3.0$ ), supersaturated ( $D > 3.0$ ), and clustered or irregular intensity with local  $D > 3.0$  and mean  $D < 3.0$ . Apparently, the above outlined models, cannot explain the supersaturated class that is found in various geological settings. A possible mechanism that could fracture the layer at supersaturated intensity is outlined below.

### Mechanisms of high density fracturing

Dynamic fracturing is a nonlinear process in which a tensile fracture propagates at high velocities that approach the Raleigh wave velocity,  $V_R$ , of the host material (Freund, 1990). Dynamic fracturing is associated with high fracture intensity, branching, and clustering of the fractures (Sharon and Fineberg, 1996; Fineberg and Marder 1999; Sagy et al., 2001). These features indicate that high intensity of fractures could reflect the profound increase in cumulative length (=surface area) of the secondary fractures within individual branched fractures. As the cumulative fracture length is increased by a factor of ten or more inside a cluster (see above), we anticipate that a complete "filling" of a layer by clusters (e.g., Reches et al., 2000) would generate a similar increase of the global intensity (Sagy et al., 2001). Although dynamic fracturing proved to be an effective mechanism to create dense fractures and clusters, it is probably limited to specific tectonic conditions, for example, near large faults (Sagy et al., 2001), or at impact sites (Sagy et al., 2004). These high energy environments could supply the energy that is required to create large branches and dynamic fractures.

Another mechanism for supersaturated tensile fractures and swarms was suggested by Germanovich and Diskin (2000), who showed that high fracture intensity could be induced by an extensional state of stress which develops near of free boundary, when  $\sigma_h \ll \sigma_v$ . The dynamic fracturing as well as the Germanovich and Diskin (2000) model, which allow for  $D \gg 1$ , assume elastic rheology. Yet, the anomalous high joints intensity in thick layers cannot be easily explained by either of these two mechanisms, and further research is required to solve this enigma.

## Acknowledgements

Discussions with Jay Fineberg, Izhak Roman, Gil Cohen and Shmuel Rubinstein are greatly appreciated. The reviews by Amotz Agnon and Yossi H. Hatzor significantly improved the manuscript. The study was supported by the US-Israel Binational Science Foundation (grant 98-135), and the Israel Science Fund (grant 175-02).

## References

- Bahat, D. 1991. *Tectonofractography*, Springer-Verlag, Berlin, 354 pp.
- Bai, T., Pollard, D.D. 2000. Fracture spacing in layered rocks: a new explanation based on stress transition. *J. Struct Geol.*, 43-57.
- Becker, A., Gross M.R. 1996. Mechanism for joint saturation in mechanically layered rocks: an example from southern Israel. *Tectonophysics*, 257, 223-237.
- Byerlee, J.D. 1978. Friction of Rocks, *Pure and Applied Geophys.* 116, 615-626.
- Engelder, T., Gross, M.R., Pinkerton, P. 1997. An analysis of joint development in thick sandstone beds of Elk basin anticline, Montana-Wyoming. in Hoak, T. E., Klawitter, A. L. and Blomquist, P. K., (eds.), *Fractured reservoirs: characterization and modeling*. Rocky Mount. Assoc. Geol., 4-21.
- Fineberg, J., Marder, M. 1999. Instability in dynamic fracture. *Phys. Rep.*, 313, 2-108.
- Finno, R, J., 2002, Evaluation of Capacity of Micropiles Embedded in Dolomite, Tech. Rep. No. A433, Northwestern Univ., Chicago.
- Freund, L.B., 1990. *Dynamic Fracture Mechanics*. Cambridge Univ. Press, 563 pp.
- Garrett, K.W., Baily, J.E., 1977. Multiple transverse fracture in 90° cross-ply laminates of a glass-reinforced polyester. *J Material Sci.*, 12, 157-168.
- Germanovich, L.N., Dyskin, A.V. 2000. Fracture mechanisms and instability of openings in compression. *Int. J. Rock Mech. Min.*, 37, 263-284.
- Germanovich, L. N., Astakhov, D. K. 2004. Stress-dependent permeability and fluid flow through parallel joints *J. Geophys. Res.*, 109 (B9): Art. No. B09203
- Ghosh, S. K., 1968. Experiments of buckling of multilayers which permit interlayer gliding. *Tectonophysics*, 207-249.
- Gross, M.R. 1993. The origin and spacing of cross joints; examples from the Monterey Formation, Santa Barbara coastline, California. *J. Struct Geol.*, 15, 737-751.
- Gross, M.R. Fischer, M.P., Engelder, T., Greenfield, R.J. 1995. Factors controlling joint spacing in interbedded sedimentary rocks; integrating numerical models with field observations from the Monterey Formation, USA. in: Ameen, .M. S. (ed.), *Fractography: fracture topography as a tool in fracture mechanics and stress analysis: Geol. Soc. Special Pub.*, 92, 215-233.
- Hobbs, D.W. 1967. The formation of tension joints in sedimentary rocks; an explanation. *Geol. Mag.*, 104, 550-556.
- Ji, S., Zhu, Z., Wang, Z. 1998. Relationship between joint spacing and bed thickness in sedimentary rocks: effects of interbed slip. *Geol. Mag.*, 135, 637-655.
- Kelly, A., Tyson, W. R. 1965. Tensile properties of fiber-reinforced metals: Copper/Tungsten and Copper/Molybdenum. *J. Mech. Phys. Solids*, 13, 329-350.
- Ladeira, F. L., Price, N. J. 1981. Relationship between fracture spacing and bed thickness. *J. Struct. Geol.* 3, 179-183.
- McQuillan H., 1973. Small-scale fracture density in Asmari Formation of southwest Iran and its relation to bed thickness and structural setting. *Am. Assoc. Petrol. Geol. Bull.*, 57, 2367-2385.
- Narr, W., Suppe, J. 1991. Joint spacing in sedimentary rocks. *J. Struct. Geol.*, 13, 1037-1048.
- Price, N. J. 1966. *Fault and joint development in brittle and semi-brittle rock*. Oxford, England, Pergamon press, 176 pp.
- Putot, C., Chastanet, J., Cacas, M.C., Daniel, J.M. 2001. Fractography in sedimentary rocks: Tension joints sets and fracture swarms. *Oil Gas. Sci. Technol.*, 56, 431-449.
- Reches, Z. 1972. Jointing in the Hazera and Hathira monoclines, northern Negev, M.Sc. thesis, Hebrew University, Jerusalem, (Hebrew with Abstract in English).

- Reches, Z. and Johnson, A. M., 1976. A theory of concentric, kink and sinusoidal folding and of monoclin flexuring of compressible, elastic multilayers; VI, Asymmetric folding and monoclin kinking. *Tectonophysics*, 35, 295-334.
- Reches, Z. 1998. Tensile fracturing of stiff rock layers under triaxial compressive stress states. *J. Rock Mech. Min. Sci.*, 35, 456-457.
- Reches, Z., Baer, G., Hatzor, Y. 1992, Constraints on the strength of the upper crust from stress inversion of fault slip measurements, *J. Geophys. Res.*, 97, 12,481-12,493.
- Reches, Z., Sagy, A., I, Roman. 2000. Dynamic fracturing web page at: <http://earth.es.huji.ac.il/reches/dynamic/>
- Rives, T., Razack, M., Petit, J.P., Rawnsley, K.D. 1992. Joint spacing: analogue and numerical simulations. *J. Struct. Geol.*, 14, 925-937.
- Roman, I., Krishnamurthy, S., Miracle, D.B. 1992. Interfacial shear properties and acoustic emission behavior of model aluminum and titanium matrix composites. *Proc. 4th Int. Symp. Acoust. Emiss. Compos. Mater.*, ASNT, Seattle, 109–114.
- Sagy, A. 1999. Jointing and faulting processes along the western margins of the Dead Sea basin. M.Sc Thesis, Heb. Univ. Jerusalem, 45 pp. (in Hebrew, English abstr.).
- Sagy, A., Reches, Z., Roman, I. 2001. Dynamic fracturing; field and experimental observations. *J. Struct. Geol.*, 23, 1223-1239.
- Sagy, A., Reches, Z. & Agnon. A. 2003. Hierachic 3D architecture and mechanics of the margins of the Dead Sea pull-apart. *Tectonics*, 22, 1, TC001323.
- Sagy, A., J. Fineberg, and Z. Reches, 2004, Shatter cones: rapid branched fractures formed by shock impact. *J. Geophy. Res.* 109, (B10) 209, 20 p.
- Sharon, E., Fineberg J. 1996. Microbranching instability and the dynamic fracture of brittle materials. *Physical Review*, 54, 7128-7139.
- Sowers, G. M. 1973. Theory of Spacing of Extension Fracture. *Engineering Geology Case Histories*, 9, 27-53.
- Wu, H., Pollard, D.D. 1995. An experimental study of the relationship between joint spacing and layer thickness. *J. Struct. Geol.*, 17, 887-905.
- Zoback, M.L., 1992, 1st-order and 2nd-order patterns of stress in the lithosphere - the world stress map project. *J. Geophy. Res.* 97, 11703-11728.

### Figure captions

Fig. 1. A two-dimensional section of a fractured brittle layer between two ductile layers (a).  $h$ -thickness of the brittle layer;  $S$  – the spacing between joints;  $\sigma_v$  and  $\sigma_h$  are remote stresses in extensional tectonic regime. **b)** The dependence of the distance between joints ( $S$ ), on the increasing shear stress ( $\tau_y$ ) is conceptually demonstrated, following Kelly and Tayson (1965). Fracturing process within the brittle material will stop at  $S_C$ , (equation 2) when the shear stress which are required to create new fractures in the brittle material is equal to the shear strength of the contacts ( $\tau_{yc}$ ).

Fig. 2. Joint intensity in the western margins of the Dead Sea basin. **a)** Measured joint intensity ( $D = h/S_m$ ) in dolostone layers divided into three groups: Group A of dominant joint sets in layers of  $h < 0.5$  m (open squares); Group B of secondary joint sets in the same layers (solid diamonds); Group C of joint sets in layers of  $h > 0.75$  m (open triangles). **b)** Predictions of the present model (see text) for the saturation joint intensity ( $D_S$ ) in layered rocks as function of the burial depth. Calculated for the parameters estimated for the western margin of the Dead Sea (see text):  $T = 7.5$  Mpa,  $a = 0.85$ , and the marked curves of  $\sigma_h/\sigma_v = 0.3, 0.5$  and  $0.7$ .

Fig. 3. **a)** Measured joint and fracture intensity in field and experiments. Dotted zone at  $1.0 < D < 3.0$  is the range of intensities predicted by the models (see text). Studies are divided into three groups, with  $D < 3$  for the undersaturated group,  $1 < D < 3$  for the saturated group and  $D > 3$  for supersaturated cases (see text). [Data sources: 1. Wu and Pollard, (1995); 2. Narr and Suppe, (1991); 3. Garrett and Bailey, (1977); 4. Ji et al., (1998); 5. Engelder et al., (1997); 6. Gross et al., (1995); 7. Wu and Pollard, (1995); 8. Narr and Suppe, (1991); 9. Gross, (1993); 10. Huang and Angelier, (1989); 11. Price, (1966); 12. McQuillan, (1973); 13. Becker and Gross, (1996); 14. Reches, (1998); 15. Reches, (1972); 16. Ladeira and Price, (1981); 17-18. Sagy et al., (2001)]. **b)** A scheme of the unsaturated (I), saturated (II), supersaturated (III), and clustered classes (IV).

Fig. 4. Field examples for supersaturated jointing in layered carbonate rocks. **a)** Joints observed on the upper surface of limestone layer; Carmel Formation, Cedar Mountain, Utah, with width  $h = 0.1$  m and mean spacing  $S_m \approx 3$  mm, and  $D \approx 33$ . **b)** View on joints in dolomite layers, Ein-Gedi area, western margin of the Dead Sea basin. The mean spacing in the 3.0 m thick bottom Layer,  $\approx 0.15$ m.

Fig 5. Experimental fracturing in layered composites subjected to layer parallel extension (after Sagy et al., 2001). **a)** Sample set-up that includes a brittle epoxy layer (1mm thick) that cements two thick polycarbonate plates (3mm thick each). External dimensions are 200 x 30 x 7 mm; Aluminum spacers replace the epoxy where the loading frame grippers are tightened on the sample. **b)** Map view of the tensile fractures (bright lines) in the epoxy layer as observed through the transparent polycarbonate layer; extension is horizontal. Left: Close-up view of a single branching fracture. Right: Close-up view of a single clustering fracture. The final density of  $D \approx 10$  results from the high density inside the clusters and partly overlaps between clusters (Sagy et al., 2001).

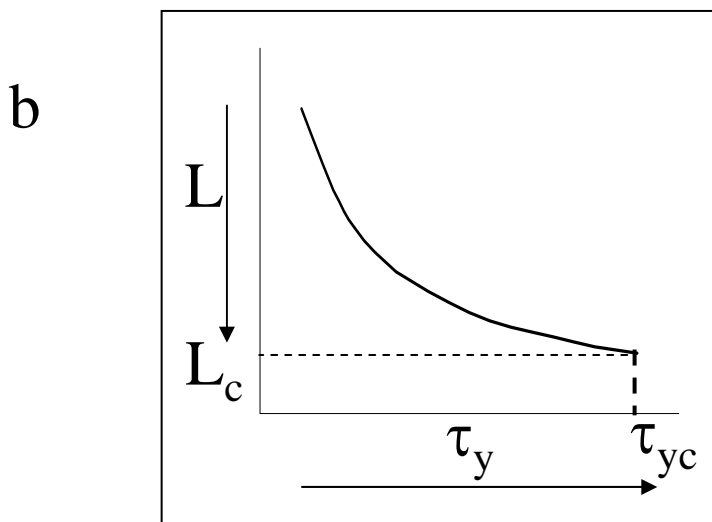
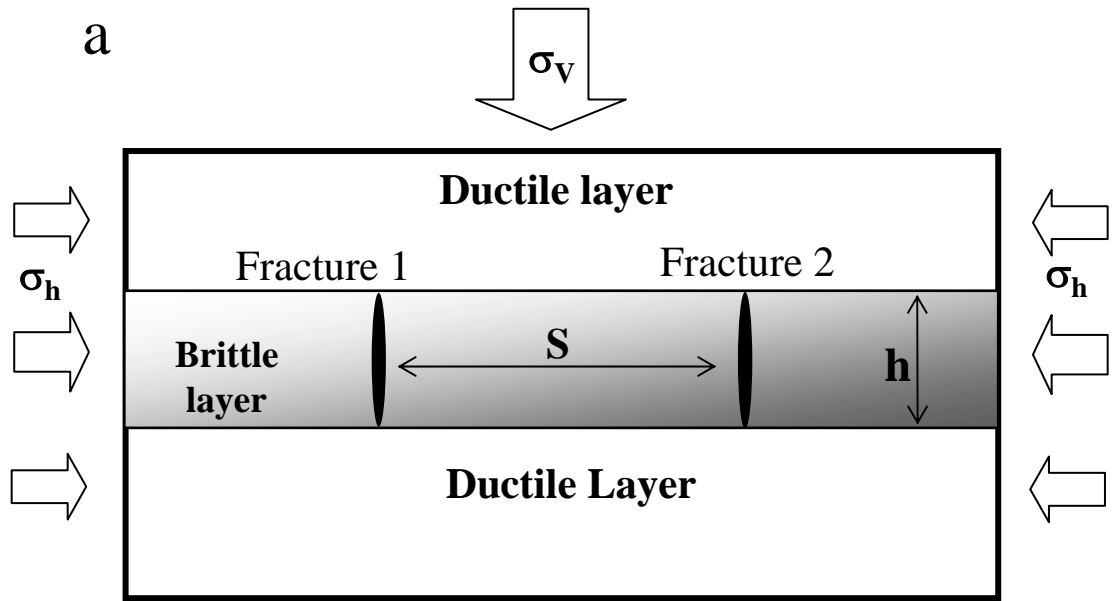


Figure 1

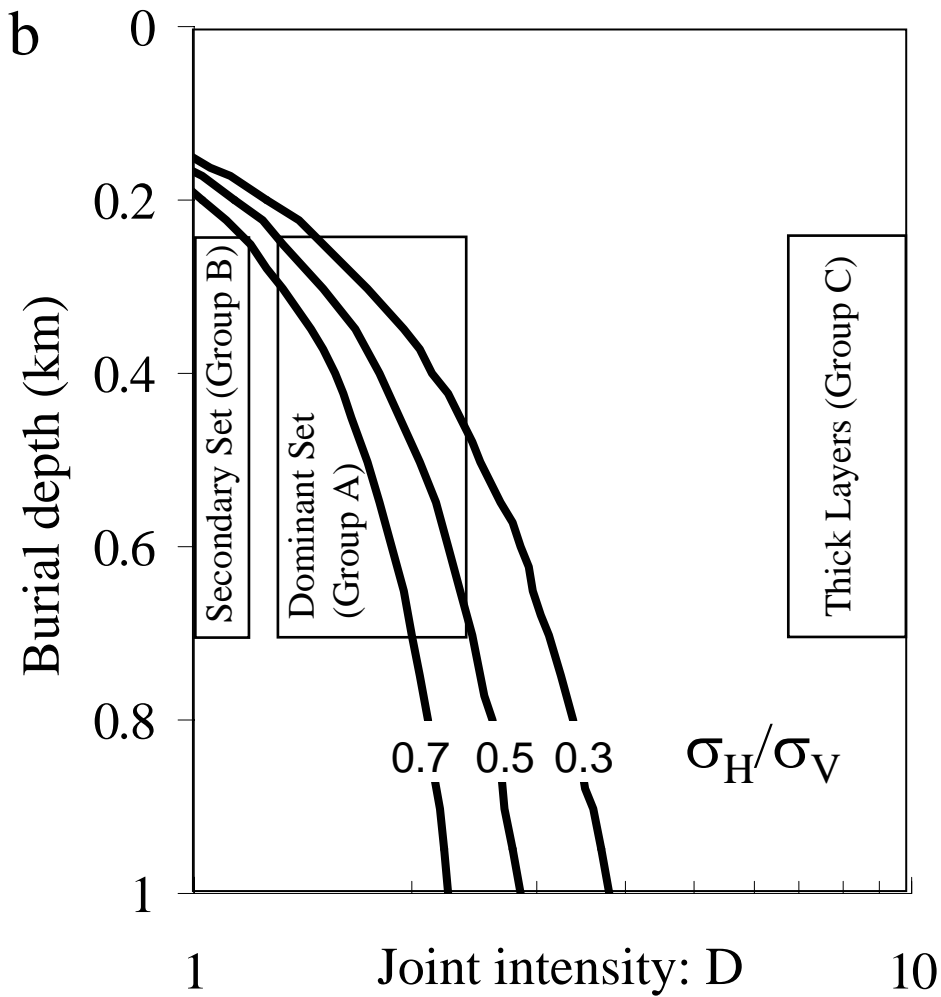
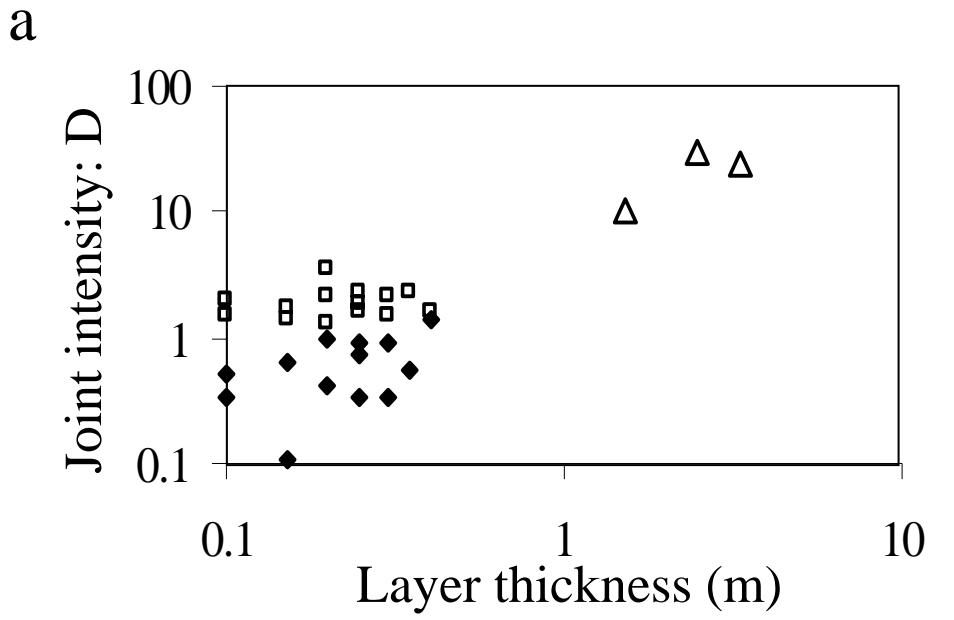


Figure 2

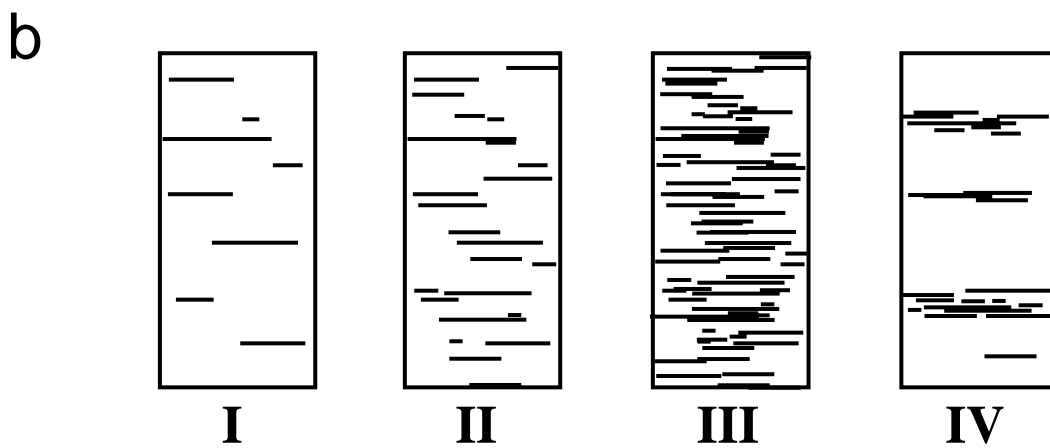
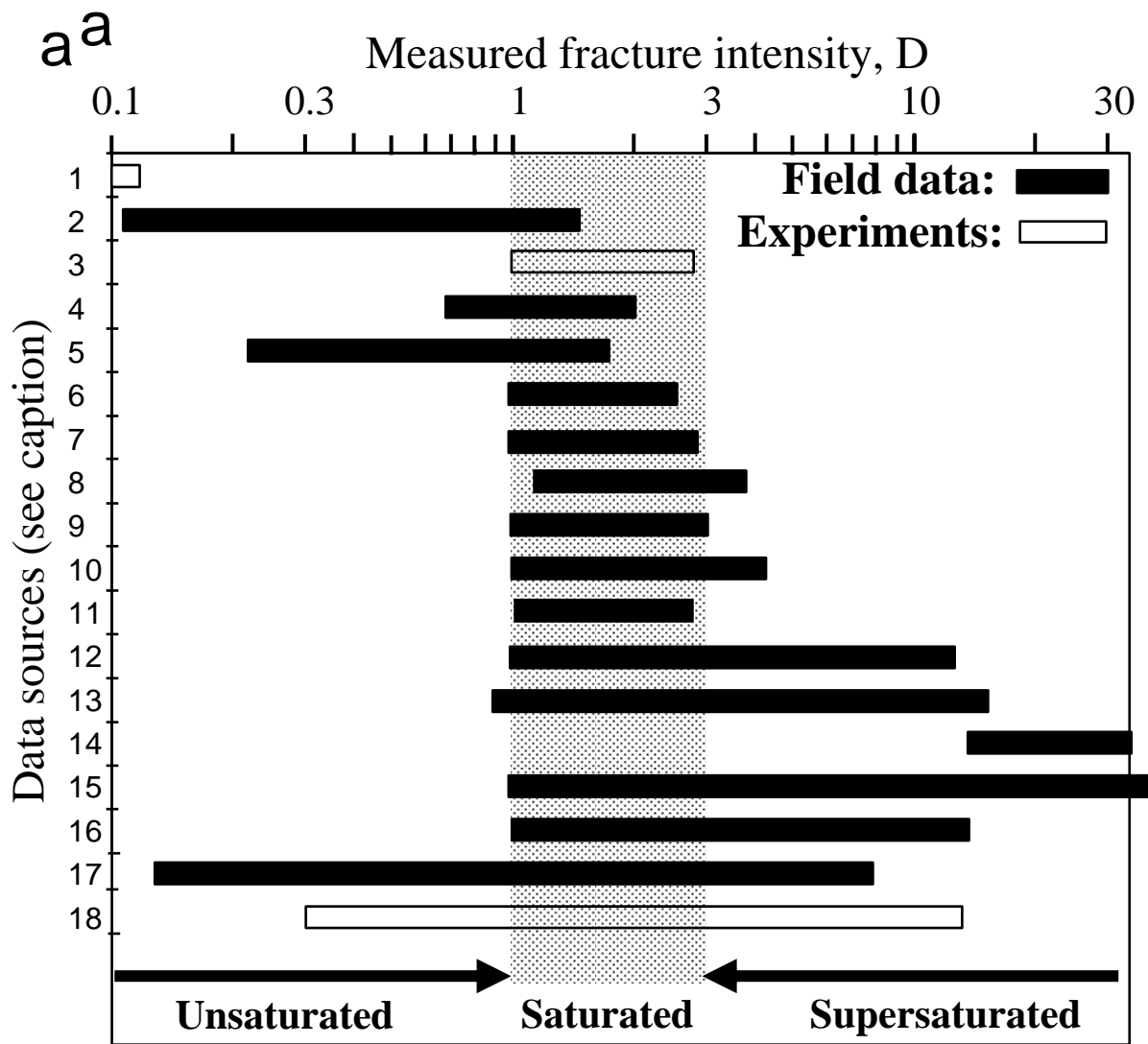
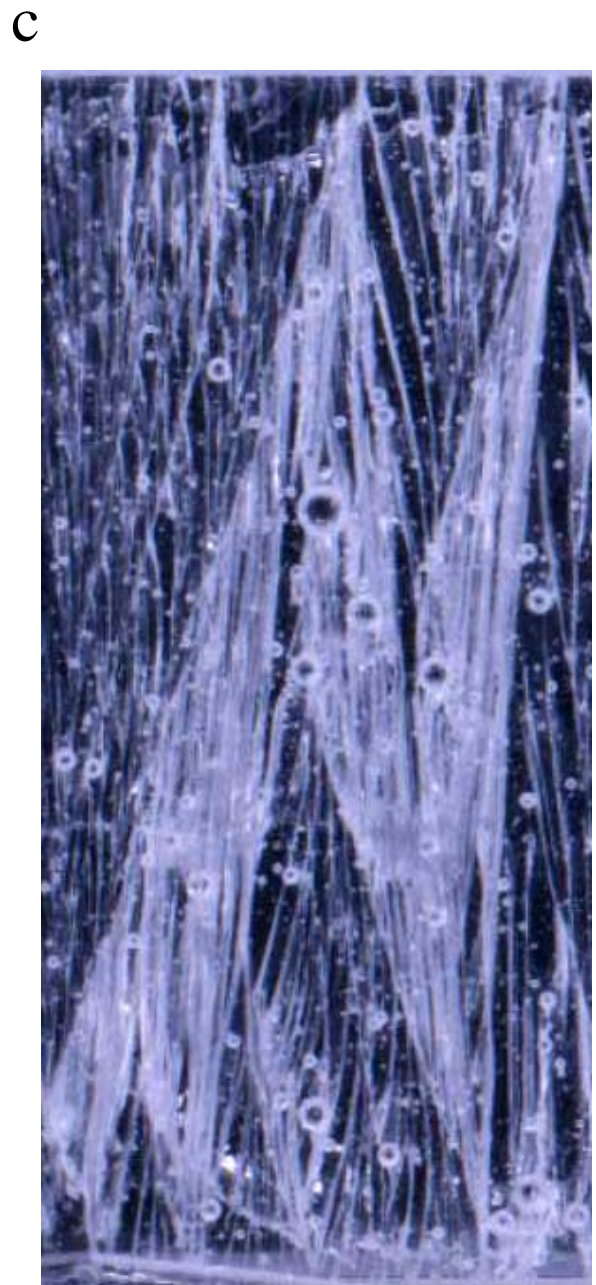
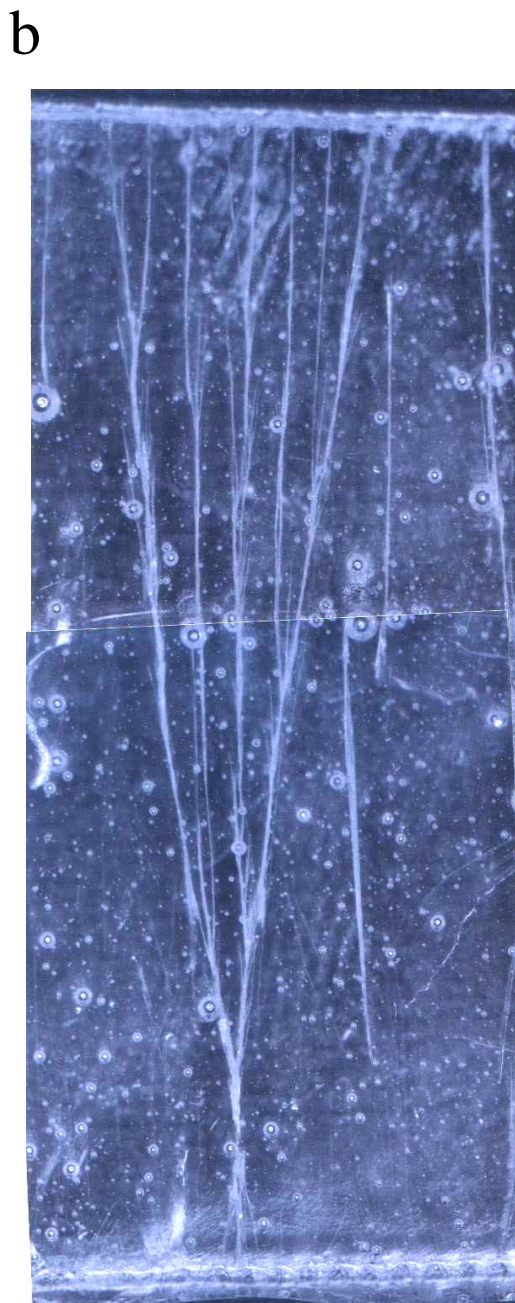
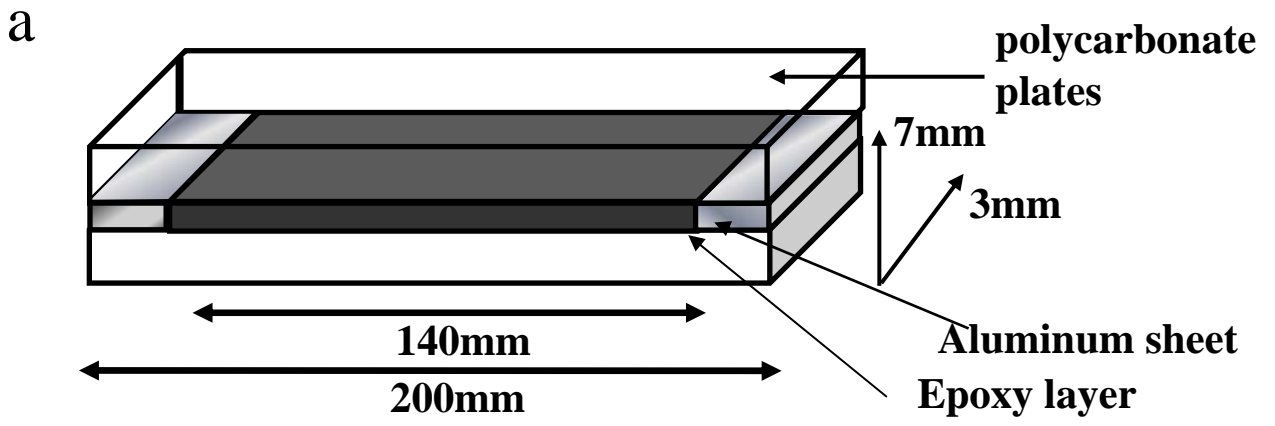


Fig. 3



Figure 4



10mm

Figure 5